Experimental Heat Transfer, 18:201–222, 2005

ISSN: 0891-6152 print/1521-0480 online
DOI: 10.1080/08916150500201529

HIGH SPEED VISUALIZATION AND DYNAMIC MEASUREMENT OF HEAT DRIVEN PUMPS

X. Shi and J. L. Xu
Guangzhou Institute of Energy Conversion, Chinese Academy of Sciences, Guangzhou, P.R. China

We provide the high speed flow visualization and dynamic measurement results for the U-shaped and the inverted U-shaped heat driven pumps. The U-shaped heat driven pumps at the high heating powers consist of a succession of tiny bubble nucleation, growth and coalescence process. Once the "larger" spherical bubble or the bubble slug forms, it expands quickly in both upstream and downstream directions. The increased pressure leads to the liquid discharge through the outlet check valve. When the advancing vapor/liquid interface reaches a higher position in the vertical discharge branch, the condensation heat transfer in the discharge branch shrinks the bubble slug, leading to the decreased pressure and initiating the open of the inlet check valve. Thus the fresh liquid can be sucked into the system. Heat driven pumps operating at the low heating powers display the similar process. However, two major differences are identified: (1) A full cycle includes a set of positive pressure pulses corresponding to a set of tiny bubble nucleation, growth and coalescence process in each substage. Only at the end of the cycle, an apparent negative pressure pulse is created. (2) For each substage in each cycle, when the newly formed bubble slug is chasing the ahead "old" bubble slug, the deformed liquid bridge is formed due to the gravity force effect. When the two bubble slugs are merging together, a wave vapor/liquid interface occurs along the bottom of the capillary tube. For the inverted U-shaped heat driven pumps, there are fewer positive pressure pulses included, corresponding to lesser number of new bubble nucleation, growth, and coalescence process. The bubble slug in the capillary tube is very standard with the smooth vapor/liquid interface. The cycle periods and the pumping flow rates are given versus the heating powers.

Keywords heat driven pump, dynamic measurement, high speed flow visualization

1. INTRODUCTION

A heat driven pump can lift liquid from a lower position to a higher position while receiving heat without mechanical rotating components. It has a simple structure that consists of two miniature/micro check valves incorporating the heat receiving piece. The two check valves specify the one-way flow direction of the fluid. Figure 1 illustrates the heat driven pump and the corresponding experimental setup used in the present article. Liquid is stored in the inlet and outlet beakers. Initially the whole loop is charged with liquid without the non condensable gas. When heating power is applied on the horizontal heating branch, liquid inside the capillary tube of the horizontal branch is heated from

Received 9 September 2004; accepted 24 May 2005.
Address correspondence to J. L. Xu, Guangzhou Institute of Energy Conversion, Chinese Academy of Sciences, Wushan, Nengyuan Road, Guangzhou, 510640, P.R. China. E-mail: xujl@ms.giec.ac.cn

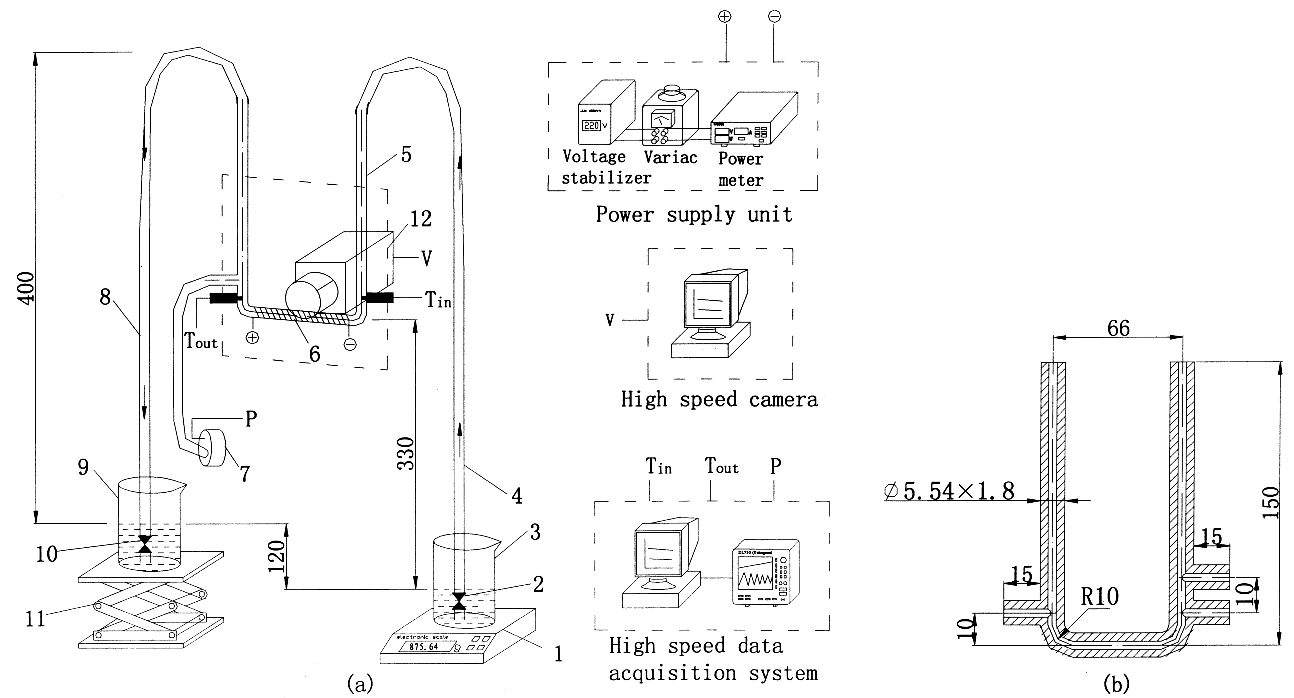

Note: All dimensions are in millimeters

1. Electronic scale
2. Inlet check valve
3. Inlet beaker
4. Suction branch
5. U-shaped capillary glass tube
6. Heating wire
7. Pressure transducer
8. Discharge branch
9. Outlet beaker
10. Outlet check valve
11. Lifter
12. High speed camera system

Figure 1. Experimental setup of the U-shaped heat driven pump.

the subcooled liquid state to the saturation. The continuous heating results in the boiling process, leading to the pressure increase inside the loop and the fluid can be discharged through the outlet check valve. Meanwhile when the expanded two-phase mixture is flowing upward in the vertical discharge branch, the vapor is partially condensed between the saturated vapor and the subcooled liquid, leading to the pressure decrease thus the fresh liquid can be sucked into the system, a new cycle starts. The device works in terms of such dynamic process periodically.

A heat driven pump is a kind of passive cooling device that does not need additional power to circulate the flow rate around the loop. In ground environment with gravity acceleration, most of the passive cooling device, such as heat pipes, can only be applied when the heating section is relatively lower than the heat sink. Even though the counter-current flow rate inside heat pipes is mainly created by the capillary pressure in the porous media or micro grooves, gravity force has influences on the thermal performance of such devices, to some extent. The thermal performance of the heat pipes becomes worse when the inclination angle is increased. Such limitation does not exist for the heat driven pump due to that the process is controlled by the boiling and condensation inside the tubes, physically. This behavior is attractive for the real cooling applications because the heat receiving piece and the heat dissipation piece (heat sink) can be located anywhere without any limitation. Besides, heat can be transferred very far away without losing any thermal performance. Heat driven pump has a good potential that can be used in the space technology under the micro gravity environment.

Yamamoto et al. [1, 2] demonstrated the heat driven pump design using the glass tube with the inside diameter of 11.5 mm. They reported the preliminary results such as the flow rate is increased with increasing the heating power. Takamura et al. [3, 4] fabricated the similar device and observed that dry-out takes place at the high heating powers. The above studies were performed at macroscale. In order to pursue the possibility that the heat driven pump can be used in the electronic cooling, Xu et al. [5] studied the heat driven pump in miniature scale with the inside diameter of 3.0 mm of the glass capillary tube. The dynamic pressure and fluid temperature pulses are recorded by a high speed data acquisition system. Indeed the thermal hydraulic parameters were repeated periodically. A one-dimensional two-phase model combined with the moving liquid/vapor interfaces was described to explain the dynamic working process [6].

Even though there are some studies on the heat driven pump, it is still a wager on its working mechanism. Thus we provided the detailed high speed flow visualization results and the dynamic measurement including pressure and fluid temperatures in this article. To the author's knowledge, the high speed flow visualization results for the heat driven pump described here were not reported previously.

2. EXPERIMENTAL SETUP

Figure 1 illustrates the experimental setup, including the inlet and the outlet beakers, the U-shaped capillary glass tube, the suction, and the discharge branches. The vertical discharge and the suction branches are made of the soft plastic tubes with the inside diameter of 3.0 mm, which were fitted with the U-shaped capillary glass tube tightly. The U-shaped glass capillary tube is shown in Figure 1b. The whole loop is arranged in the vertical plane. The inlet and the outlet beakers are full of deionized water. Initially the whole loop is charged with the deionized water without the non condensable gas.

The inlet and outlet check valves are immersed under the water surface. During the operation of the heat driven pump, the liquid surface of the inlet beaker is lower than that of the outlet one by 12 cm. The U-shaped glass capillary tube has the outer diameter of 5.54 mm with the thickness of 1.8 mm. The inside diameter of the capillary tube is 1.94 mm. On the body of the U-shaped glass capillary tube, there are three T-junctions with the inside diameter of 1.0 mm. The K-type thermocouple wires with the diameter of 0.3 mm are inserted inside the two holes thus the dynamic fluid temperatures can be measured. The third T-junction is used to connect the soft plastic tube with the pressure transducer to measure the dynamic pressure. These T-junctions are located close to the two U-bends.

The two miniature check valves have the inside diameter of 1/8 inch (3.175 mm, Cole-Parmer International, USA, U98553-20). The two valves were carefully selected to have the nearly the same parameters. They have the measured crack pressure of 300 mm H_2O. The crack pressure is defined as when the check valve should overcome the pressure drop across the two ports thus the valve can be open. Once the check valve is in open state, it does not close until the net pressure drop across its two sides becomes zero.

The heating wires were wrapped on the outer surface of the horizontal branch manually with the neighboring interval of 2.0 mm as uniform as possible. The two ports of the heating wires were connected with the power supply unit, consisting of a voltage stabilizer, variac, and power meter. The voltage stabilizer is used to stabilize the AC voltage for the output of 220 V, which is used as the input of the variac. The variac can be adjusted to obtain a desired voltage thus one can acquire a stable controlled heating power that is applied on the heating wire. The power meter measures the voltage, current, and power simultaneously. The uncertainty of the heating power is less than 0.5 W. The fluid pressure inside the capillary tube is dynamically measured by a Setra pressure transducer (Model 206), which was calibrated against a known standard and the uncertainty is less than 0.1%. The pressure data presented in this article is the pressure reference to the environment pressure. The negative value means that the absolute pressure inside the heat driven pump is less than the environment pressure. The thermocouple wires have the errors less than 0.2°C after calibration with a constant temperature bath.

The inlet beaker was weighed by a precision electronic scale, with the uncertainty of 0.01 g. Because the flow rate is very small, the pumping flow rates provided in this article are the average values obtained from the weight decrement of the inlet beaker over a certain period of time. For a new heating power, the heat driven pump was running for more than one hour to reach the steady oscillating state. The pressure and the fluid temperatures are dynamically recorded by a high speed data acquisition system (DL-750, Yokogawa, Inc., Japan) with 16 channels. The data sampling rate can be up to 500 K samples per second. In the present study we use the sampling rate of 500/s, which is fast enough to capture the dynamic pressures and temperatures.

The bubble dynamics were recorded by a high-speed digital camera (HG-100K, Redlake Inc, USA). The advanced 1.7M CMOS sensor was used, which can capture the dynamic pictures up to 10,000 frames/s, having the sensitivity of 1504 × 1128 pixels. In the present paper, at the lower heating power such as less than 30 W, the image sampling rate was selected as 500 frames/s. However, at the higher heating power larger than 30 W, the image sampling rate of 1,000 frames/s was used. At these sampling rates, the dynamic process of the heat driven pump can be continuously viewed for several full cycles. The high-speed camera is equipped with a micro leans thus a short distance around 20–30 cm between the camera lense and the flow view field is adjusted. At each run case, the U-shaped glass tube is viewed in the center part of the screen. A powerful light source with the power up to 1.5 kW is turned on to form the clear images. This is important when the sampling rate is high. The successive images can be illustrated in the PC screen frame by frame and stored in PC memory for future analysis. The time step for each continuous image is 2.0 ms and 1.0 ms, corresponding to the image sampling rates of 500 and 1,000 frames per second. The PHOTOSHOP commercial software was used to process the successive images. During the measurement, the high-speed camera and the high-speed data acquisition system were triggered on simultaneously, thus synchronous measurements were performed.

Alternatively, the high speed flow visualization of the heat driven pump using the inverted U-shaped glass tube as the test section was also tested. Figure 2 shows such arrangement. The only difference is that the glass capillary tube is inverted located in the vertical plane. The purpose of using both the U-shaped and the inverted U-shaped heat driven pumps is to verify how the gravity force affects the two-phase structure inside the pumping loop and the thermal performance.

3. RESULTS AND DISCUSSION

3.1. Visualization and Measurement Results at High Heating Powers

In one full cycle, the heat driven pump operating at high heating powers behaves a successive of bubble nucleation, growth, coalescence, liquid discharge, and suction process. Figure 3 displays the dynamic measurement results for the fluid pressure P and the inlet and outlet fluid temperatures, T_{in}, T_{out}. A full typical cycle is defined from $t = t_A$ across $t = t_B$, $t = t_C$ and ending at $t = t_D$. Correspondingly the successive images are shown in Figure 4. The detailed working process is described as follows.

3.1.1. Bubble nucleation, growth and coalescence period ($t_A < t < t_B$). At $t = t_A$, the capillary glass tube of the heat driven pump is full of liquid (see Figure 4). With time evolving ($t > t_A$), the isolated tiny bubbles begin to occur on the upper part of the horizontal capillary tube. Initially the locations of these small nucleated bubbles are close to the left elbow (the corner of the vertical discharge branch, see Figure 4 at $t = 0.134$ s). This is because such locations always have higher liquid temperatures. With time evolving the tiny bubbles are growing up, and the inside wall surface area of the capillary tube that nucleates the tiny bubbles is expanded from $t = 0$ to $t = 0.344$ s. Once the length of the tiny bubble train in the horizontal heating section reaches nearly one half of the total heating length (see Figure 4 at $t = 0.246$ s and $t = 0.344$ s), the tiny spherical bubbles that were initially nucleated near the left elbow coalescence to form a single spherical bubble whose diameter reaches the inside diameter of the capillary tube at $t = 0.452$ s (t_B). However, the other tiny bubbles are still lined up on the upper part of the capillary tube behind such "larger" spherical bubble.

It costs nearly 0.452 s from t_A to t_B. In such a period, even though the bubble nucleation, growth, and coalescence process takes place, the vapor void fraction in the capillary tube is still small and the fluid pressure keeps nearly constant (see Figure 3). Besides, the liquid in the two vertical branches are nearly stationary, thus the liquid temperatures are slightly decreased due to the heat loss to the environment. The two check valves are closed.

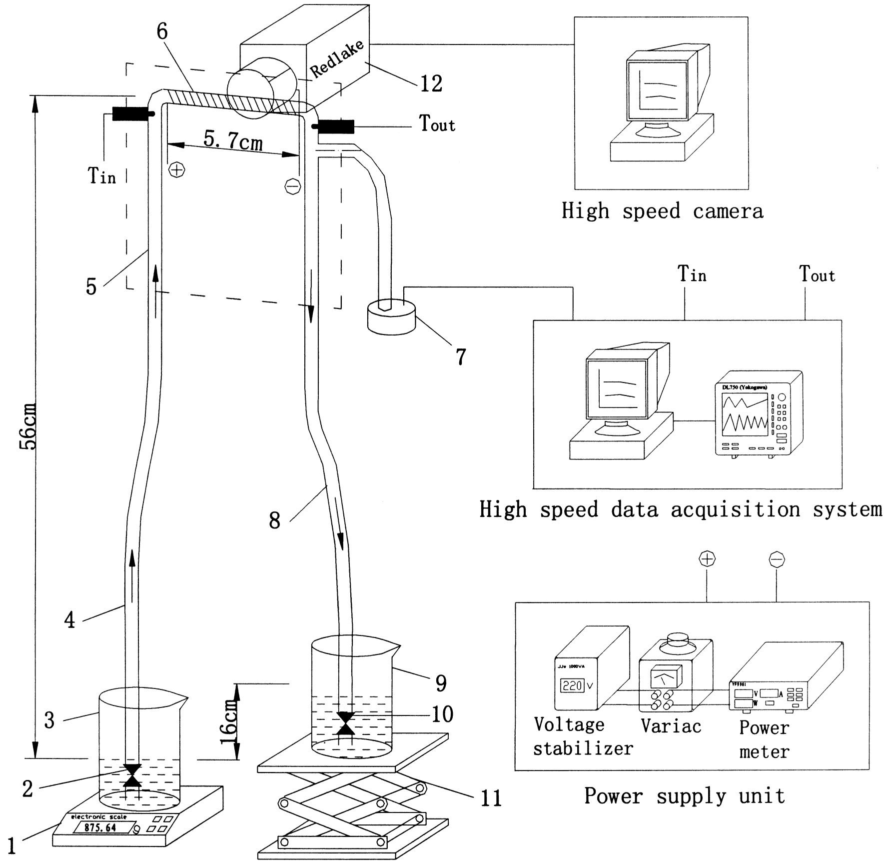

1. Electronic scale
2. Inlet check valve
3. Inlet beaker
4. Suction branch
5. U-shaped capillary glass tube
6. Heating wire
7. Pressure transducer
8. Discharge branch
9. Outlet beaker
10. Outlet check valve
11. Lifter
12. High speed camera system

Figure 2. Experimental setup of the inverted U-shaped heat driven pump.

It is observed that once the "larger" spherical bubble is formed, it can have a sharp expansion and absorb the neighboring small bubbles to form the bubble slug. Thus the fluid pressure begins to have a sharp increase at $t = t_B$.

It is noted that the fluid inside the capillary tube is stationary. Under such a condition, heating applied on the horizontal branch results in the natural circulation in the cross section of the capillary tube. The "hotter" liquid always stays on the upper part of the capillary tube. This is the reason why the tiny bubbles are always initially nucleated on the upper part of the horizontal heating section.

3.1.2. Elongated bubble slug and liquid discharge period ($t_B < t < t_C$). Following $t > t_B$, generally the bubble slug is quickly expanding in both upstream and downstream directions. In this period, the advancing vapor/liquid interface is successively moving in the left U-bend and flowing upward in the vertical discharge branch.

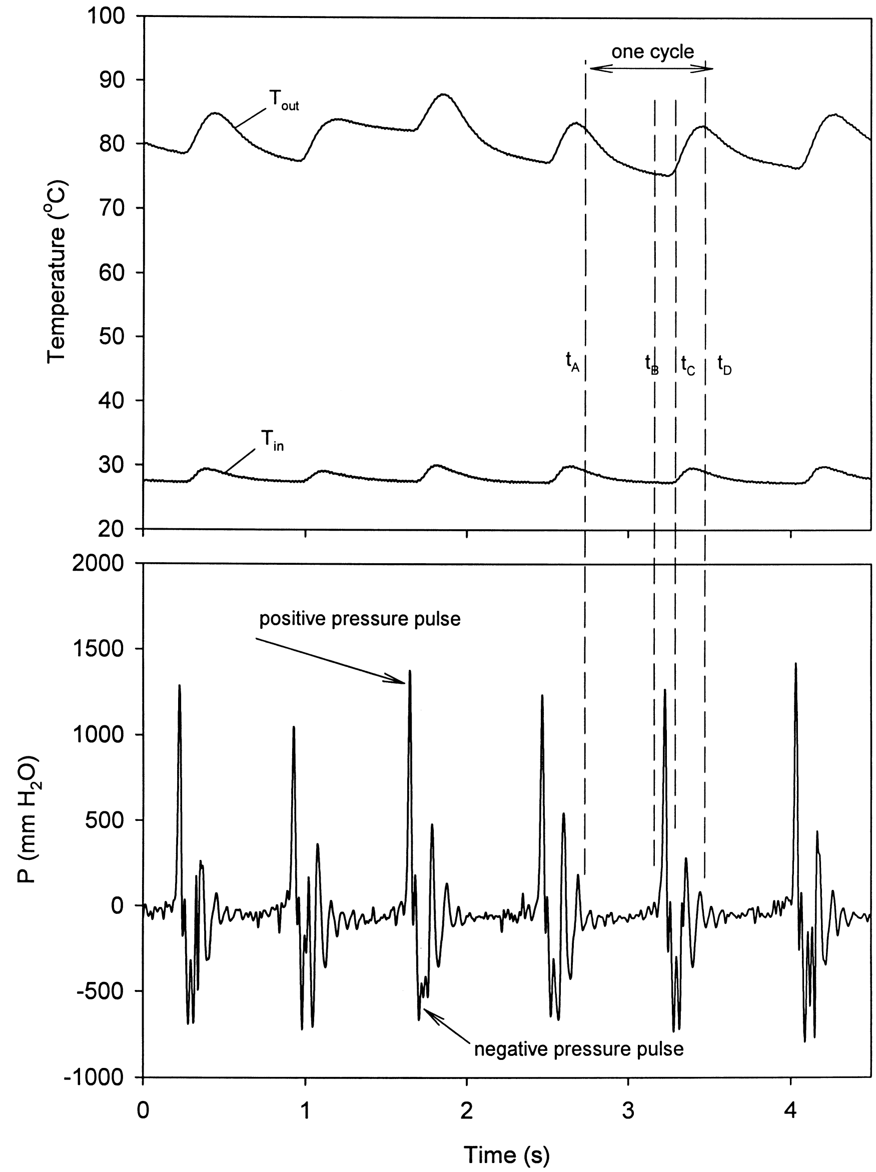

Figure 3. Dynamic recordings of pressures and fluid temperatures versus time for the U-shaped heat driven pump at the heating power of 40.0 W.

Such interface has the maximum position at $t = 0.544$ s (t_C). The other vapor/liquid interface is flowing toward the right U-bend (the vertical discharge branch). From t_B to t_C only lasts 0.09 s, in which a positive pressure pulse is formed (see Figure 3). The pressure inside the heat driven pump depends on the boiling heat transfer in the horizontal heating section and the condensation heat transfer between the saturated vapor and the subcooled liquid in the vertical discharge branch. Just beyond t_B, the sharp increased

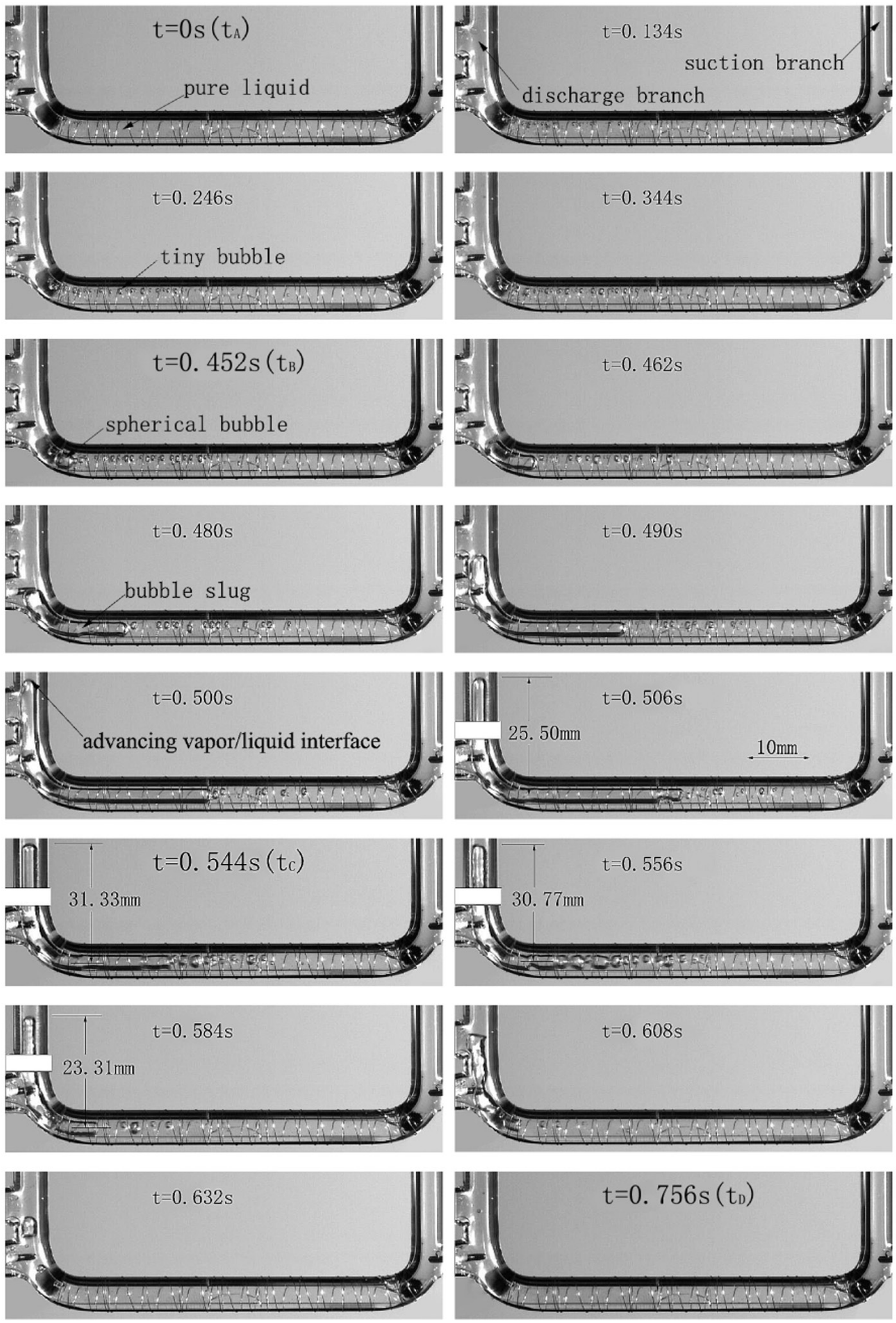

Figure 4. High-speed flow visualization of the U-shaped heat driven pump at the heating power of 40 W.

pressure is mainly controlled by the bubble slug expansion in the horizontal heating section. Inversely, once the vapor/liquid interface reaches a higher level in the vertical discharge branch, the interface condensation heat transfer in the vertical discharge branch results in the sharp decrease of the pressure from the peak value. In such a short period, the net pressure inside the heat driven pump exceeds the crack pressure of the outlet check valve, leading to the open of the valve and liquid is discharged to the outlet beaker. In all the cases tested, the front of the vapor/liquid interface never reaches the outlet check valve. Thus the fluid that is discharged to the outlet beaker is the liquid, not the vapor or vapor/liquid mixture.

The heat driven pump system depends on the boiling heating transfer in the horizontal heating section and the condensation heat transfer in the vertical discharge branch. Boiling always induces the pressure increase while condensation leads to the pressure reduction. The net pressure in the heat driven pump is balanced between the above two effects. The net pressure changing rate consisting of the two parts is written as:

$$\frac{dP}{dt} = \left.\frac{dP}{dt}\right|_{boil} + \left.\frac{dP}{dt}\right|_{con}, \tag{1}$$

where $\frac{dP}{dt}$ is the net pressure change rate, and $\frac{dP}{dt}|_{boil}$ and $\frac{dP}{dt}|_{con}$ are the pressure change rates induced by boiling and condensation heat transfer, respectively. If the net pressure change rate is positive, the pressure can be increased versus time thus there is a possibility to initiate the open of the outlet check valve, which exists in the period of $t_B < t < t_C$.

3.1.3. Bubble slug contradiction and liquid suction stage ($t_C < t < t_D$). At $t = t_C$, the bubble slug in the vertical discharge branch has the highest position. At this time, because the bubble slug has the largest surface area (the core of the bubble slug) that contacts the subcooled liquid film surrounding the vapor core in the vertical discharge branch, the negative pressure change rate induced by the condensation heat transfer in the vertical discharge branch exceeds the positive one induced by the boiling in the horizontal heating branch. Thus the pressure has a sharp negative pressure pulse, initiating the open of the inlet check valve and the fresh liquid is sucked into the system. The bubble slug is shortened, with the vapor/liquid interface in the vertical discharge branch returns back to the left U-bend (the corner). The sucked subcooled liquid sweeps all the isolated bubble train behind the bubble slug. In addition, the vapor/liquid interface of the bubble slug in the horizontal heating section moves quickly toward the left U-bend, until all the bubbles (including the bubble slug and the isolated bubbles) disappear at $t = t_D$.

3.1.4. Summary of the working process of the heat driven pump. A heat driven pump works in the periodic mode. A full cycle consists of a successive of tiny bubble nucleation, growth, and coalescence process. Once the spherical bubble that reaches the inside diameter of the capillary tube, it expands quickly in both upstream and downstream directions, with one vapor/liquid interface flushing the vertical discharge branch, and the other one moving toward the right U-bend of the vertical suction branch. The expanded bubble slug results in the liquid discharge through the outlet check valve. When the vapor/liquid interface is higher in the vertical branch, the condensation heat transfer between the saturated vapor and the subcooled liquid film domains the pressure decrease. The fresh liquid is sucked into the system and sweeps all the bubbles. The system repeats the above process periodically.

3.2. Visualization and Measurement Results at Low Heating Powers

A heat driven pump using the U-shaped capillary tube operating at lower heating powers also displays the cycle behavior, which is similar to that at higher heating powers. However, there are two new phenomena that only take place at low heating powers: one is the multi positive pressure pulse and liquid discharge phenomenon in a full cycle, the other is the wave vapor/liquid interface phenomenon on the bottom of the horizontal heating section. These special characteristics are described as follows.

3.2.1. Multi positive pressure pulse and liquid discharge phenomena in one full cycle. Figure 5 displays the dynamic measurements of pressures and fluid temperatures at the heating power of 20 W. The successive high speed images are shown in Figure 6. Again the cycle behavior appears. In a full cycle, the inlet liquid temperature behaves the uniform distribution followed by a triangular-shape distribution (see Figure 5). The outlet fluid temperature illustrates the quasi-trapezoid shape (see Figure 5). However, compared with the high heating power such as 40 W, the pressure signal displays a set of positive pulses. Only at the end of each cycle, a sharp negative pressure pulse followed by a positive pulse appears. Each positive pressure pulse indicates a bubble expansion process, leading to the liquid discharge through the outlet check valve. The negative pressure pulse at the end of the cycle corresponds to the highest position of the bubble slug in the vertical discharge branch. The strong condensation heat transfer between the saturated vapor and the subcooled liquid film surrounding the vapor core in the vertical discharge branch causes a sharp pressure decrease thus the liquid suction can be initiated.

Now we turn to analyze a succession of high-speed images that demonstrate the dynamic working process. Again a full cycle is selected starting from $t = t_A$ at which the capillary tube is full of pure liquid, and ending at $t = t_F$ at which the system returns to the single-phase liquid state (see Figure 5 for the dynamic measurements and Figure 6 for the images).

Based on the number of the positive pressure pulses, we divided a full cycle into several substages, such as $t_A < t < t_B$, $t_B < t < t_C$, $t_C < t < t_D$, $t_D < t < t_E$, and $t_E < t < t_F$. Among them in each of the former four substages, only a positive pressure pulse occurs. On the other hand, only a sharp negative pressure pulse is followed by a sharp positive pressure pulse in the last substage for $t_E < t < t_F$.

In the first substage for $t_A < t < t_B$, a successive of images (see Figure 6) show the tiny bubble nucleation, growth, and coalescence process. Once the bubble slug is formed and expands toward the left U-bend, a positive pressure pulse appears.

The second, third, and fourth substages for $t_B < t < t_C$, $t_C < t < t_D$, and $t_D < t < t_E$ repeat the similar process. Here only one of them for t_D ($t = 1.952$ s) $< t < t_E$ ($t = 3.048$ s) is described.

At the start of each substage such as at $t = 1.952$ s (t_D), the enhanced boiling heat transfer in the horizontal heating section leads to the sharp pressure increase. On the other hand, once the moving front of the bubble slug reaches a relative higher position in the vertical discharge branch, the condensation effect causes the pressure decrease, thus a positive pulse forms, which causes the liquid discharge through the outlet check valve. Because the condensation heat transfer is not strong enough to decrease the pressure to the level that can overcome the crack pressure of the inlet check pressure, the liquid suction is not initiated. Once the positive pressure pulse elapses, the location of the vapor/liquid interface of the bubble slug in the vertical discharge branch has a slight

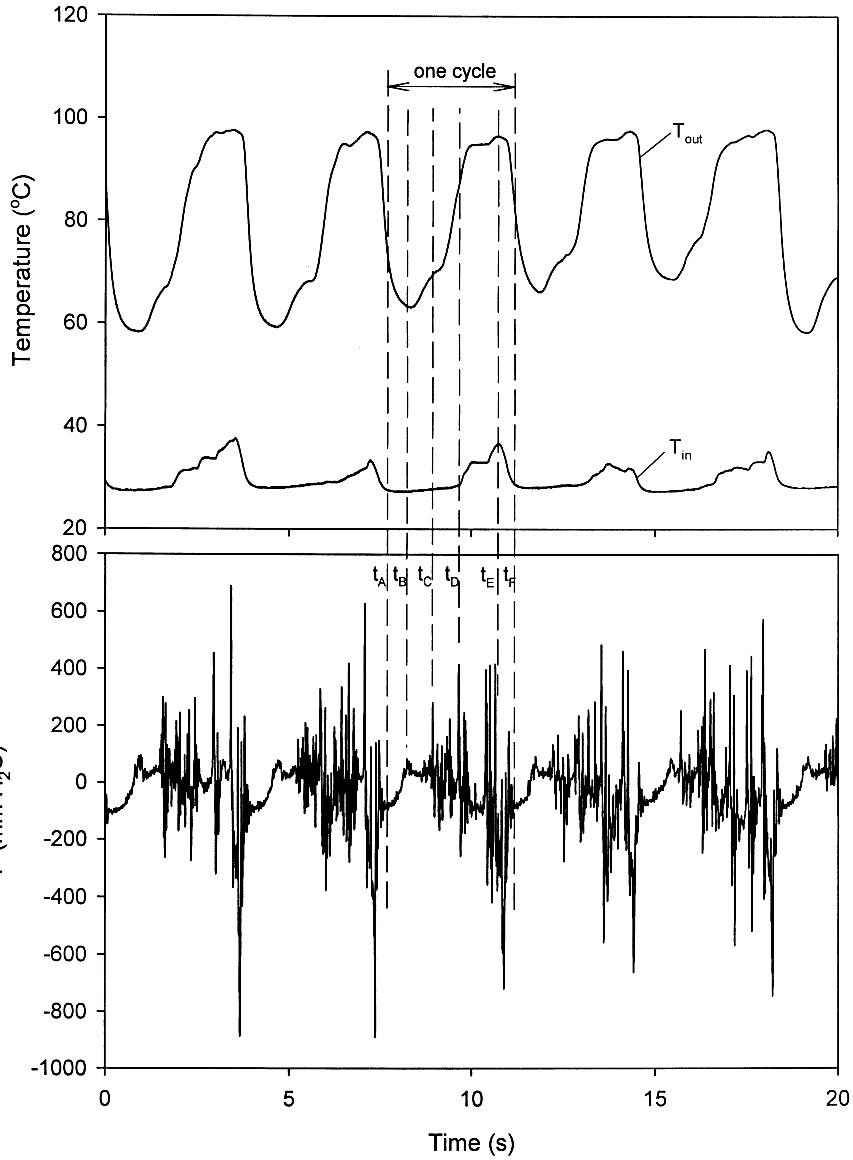

Figure 5. Dynamic measurements of the heat driven pump at the heating power of 20 W.

decrease (see images in Figure 6 from $t = 1.952$ s to $t = 2.076$ s). Meanwhile, the new tiny bubbles are nucleated on the upper part of the horizontal heating section (see image at $t = 1.952$ s). These tiny bubbles are growing up quickly and coalescence to form a new single spherical bubble whose diameter is in the order of the inside diameter of the capillary tube at $t = 2.060$ s. The continuous expansion of the spherical bubble forms a new bubble slug at $t = 2.076$ s and $t = 2.086$ s. The newly formed bubble slug chases the ahead longer bubble slug and coalesce with each other at $t = 2.120$ s.

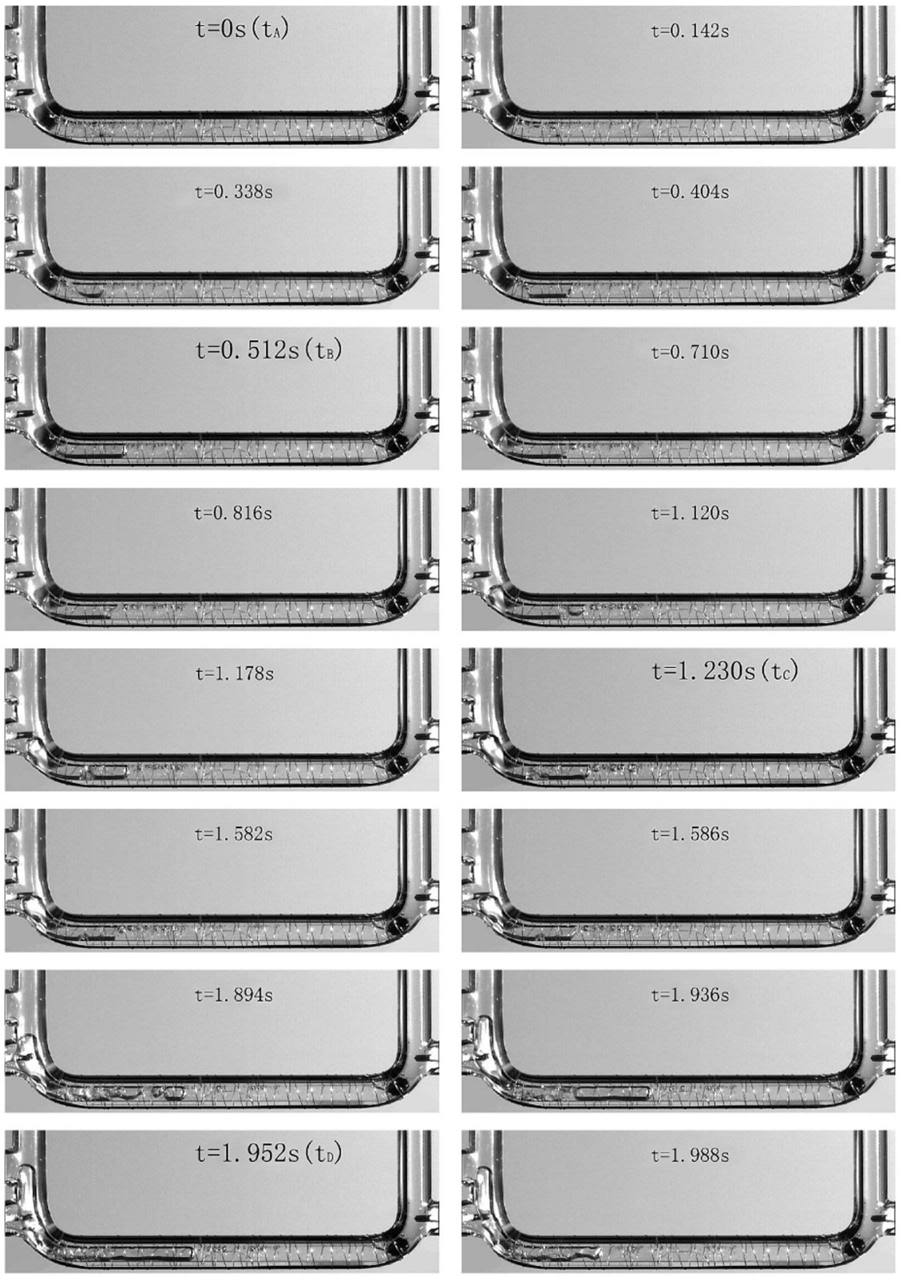

Figure 6. High-speed flow visualization of the U-shaped heat driven pump at the heating power of 20 W (*continues*).

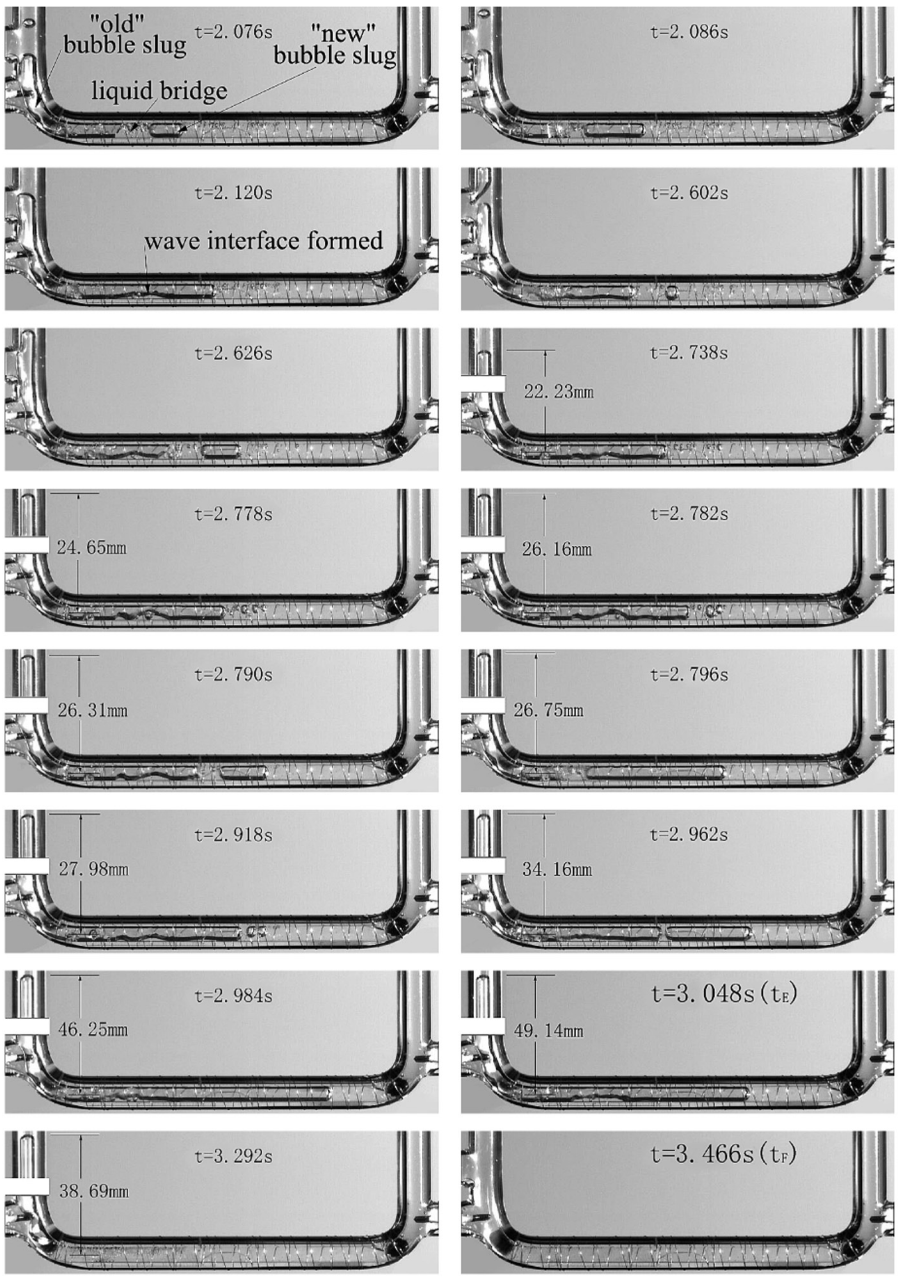

Figure 6. (*Continued*)..

Once the coalescence of the two neighboring bubble slugs occurs, the position of the vapor/liquid interface in the vertical discharge branch is increased. Following $t = 2.120$ s, the successive of new tiny bubbles nucleate, grow up, and coalescence to form a new spherical bubble. The expansion of the new bubble slug and the coalescence of the two bubble slugs repeat. For each coalescence of the two bubble slugs, the location of the vapor/liquid interface of the bubble slug in the vertical discharge branch has an increase. Such dynamic process repeats until at $t = 3.048$ s (t_E) when the bubble slug reaches the highest position of 49 mm in the vertical discharge branch.

In the early of the last substage for $t = 3.048$ s(t_E) $< t < t = 3.466$ s(t_F), the highest vapor/liquid interface of the bubble slug in the vertical discharge branch leads to the strong condensation heat transfer, resulting in a sharp negative pressure pulse. In a very short time, the inlet check valve is open to suck the fresh liquid into the system. A full cycle ends at the pure subcooled liquid state, and a new cycle begins.

3.2.2. Wave vapor/liquid interface on the bottom of the horizontal heating section. When the heat driven pump is operating at the low heating power, it is observed that during specific substage in a full cycle the bubble slug in the horizontal heating section has a wave vapor/liquid interface along the bottom of the horizontal heating section. A successive of dynamic images illustrating the formation of the wave vapor/liquid interface can be identified from $t = 2.076$ s to $t = 2.120$ s in Figure 6. In such a short period a new bubble slug is formed due to a successive of tiny bubble nucleation, growth, and coalescence process. It is observed that the newly formed bubble slug has a higher velocity than the ahead "old" bubble slug, thus the bubble slug chasing and coalescence process take place. The liquid bridge between them is compressed by the newly formed bubble slug. The gravity force of the liquid bridge will pull the liquid down to the bottom of the capillary tube. Thus a deformed trapezoid liquid bridge is formed between the two neighboring bubble slugs. When the two bubble slugs are merging together, a very thick liquid film on the bottom of the capillary tube exists. Thus the wave vapor/liquid interface is formed. The schematic illustration showing the formation of the wave vapor/liquid interface is shown in Figure 7.

3.3. Flow Visualization and Measurements for the Inverted U-Shaped Heat Driven Pump

Figures 8 and 9 show the flow visualization and the dynamic measurements for the inverted U-shaped heat driven pump at the heating power of 20 W. The right vertical branch is the discharge one, while the left one is the suction branch. Compared with the results for the U-shaped heat driven pump, the inverted U-shaped heat driven pump has the following characteristics.

The dynamic working process for a full cycle is relatively simple. There are fewer substages in a full cycle for the inverted U-shaped heat driven pump. The inlet and outlet fluid temperatures behave the trapezoid shapes, while the pressures display a couple of positive pulses. The number of the positive pressure pulses is less than that of U-shaped heat driven pump. Each positive pressure pulse corresponds to a bubble slug expansion and shrinking process. The last positive pressure pulse is followed by a negative pulse at the end of each cycle. The liquid suction is only taking place in the very narrow negative pressure pulse period.

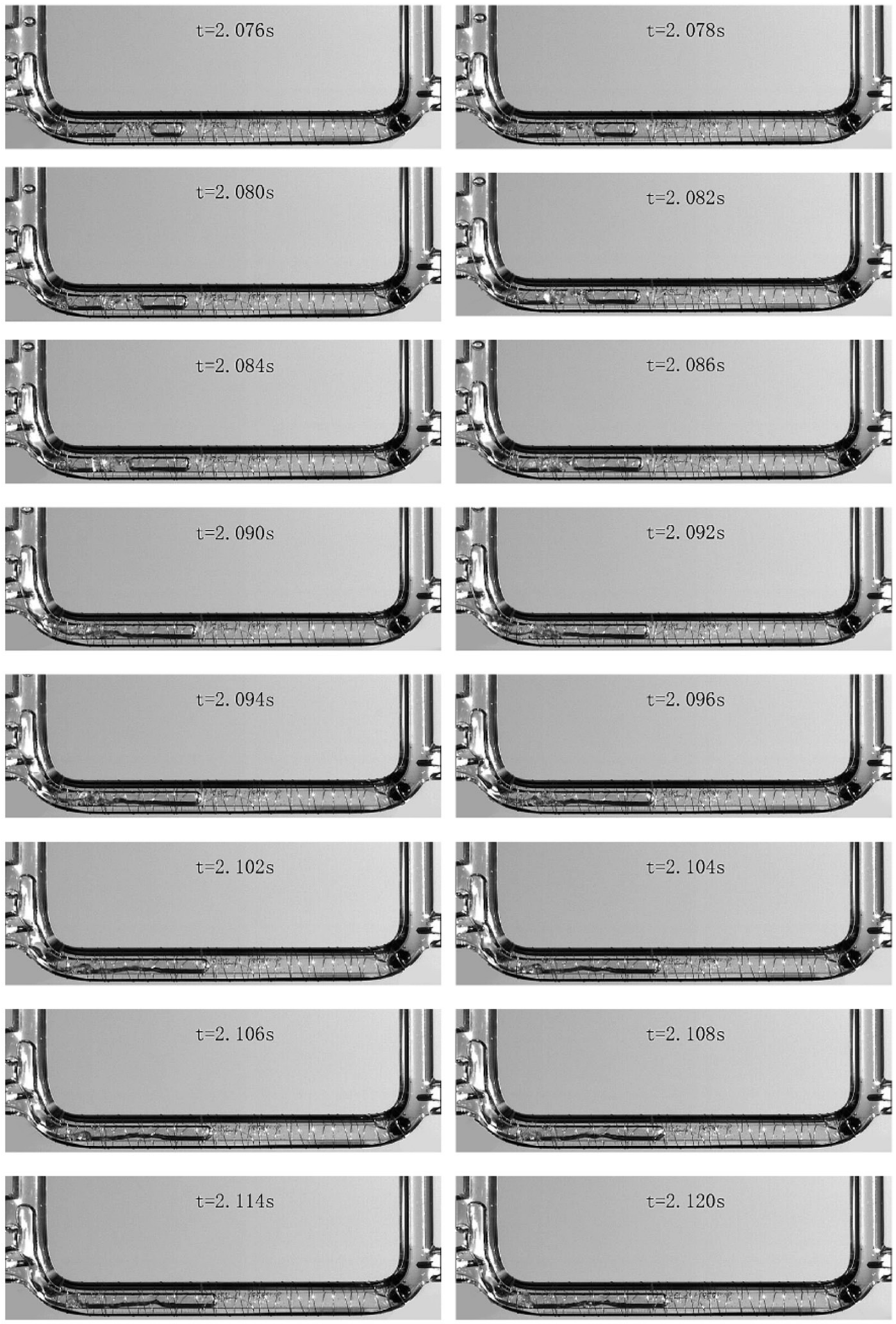

Figure 7. The successive images illustrating the formation of the wave vapor/liquid interface on the bottom of the capillary tube.

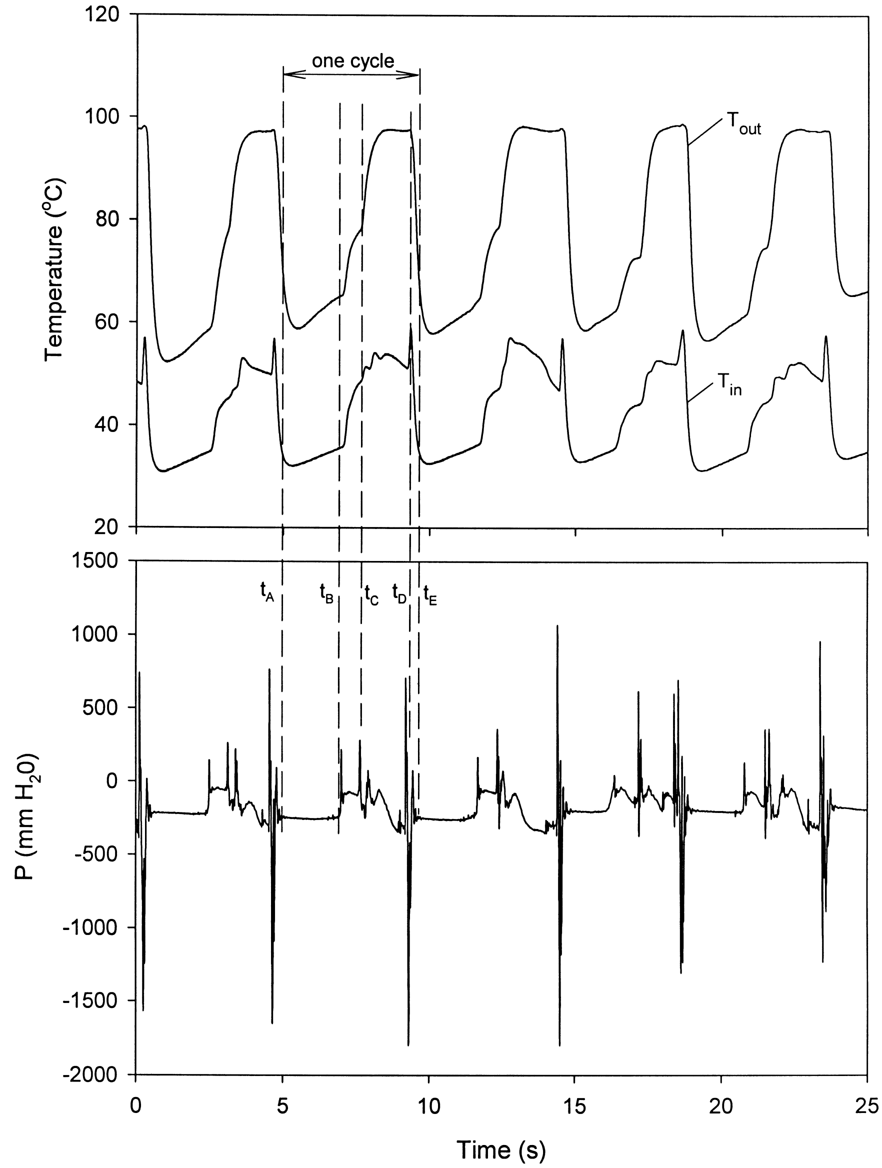

Figure 8. Dynamic measurements of the inverted U-shaped heat driven pump at the heating power of 20 W.

In contrast to the U-shaped heat driven pump, the bubble slug in the capillary tube of the inverted U-shaped heat driven pump behaves as a very normal bubble slug shape without the wave vapor/liquid interface on the bottom of the capillary tube. The typical bubble slug coalescence process can be identified from the images at $t = 2.570$ s, 2.584 s, 2.610 s, 2.618 s, and 2.632 s. During such a bubble slug chasing and coalescence process, the liquid bridge between the two bubble slugs is pushed by the newly formed bubble slug. Once the liquid bridge reaches the right U-bend, it is easy to fall down along the vertical discharge branch due to the gravity force effect. Thus it has no possibility that the liquid is falling down on the bottom of the horizontal capillary tube thus the wave vapor/liquid interface is not observed.

3.4. Pumping Performance

The pumping performance includes the cycle periods and the pumping flow rates. The cycle period is obtained from the measurements of the dynamic parameters such as pressure and fluid temperatures. Alternatively, the cycle periods can also be identified by carefully checking a successive of high speed images. These two methods are consistent with each other. The pumping flow rates are acquired by measuring the mass reduction of the inlet beaker over a given period of time. It is observed from Figure 10 that the cycle period is high at low heating power, but is decreased with increasing the heating power, indicating that the pumping process becomes fast with increasing the heating powers. It is also observed that the cycle periods for the inverted U-shaped heat driven pump is slightly longer than those of the U-shaped one at the same heating powers. The pumping flow rates are observed to be increased with the heating power linearly for both of the heat driven pumps. From the above results it is shown that the pumping performance is indeed not affected by the gravity force. The gravity force only affects on the vapor/liquid structure in the horizontal heating section.

4. WORKING PRINCIPLE AND SCALING LAW OF THE HEAT DRIVEN PUMPS

A heat driven pump is a kind of passive cooling device that can pump fluid from a lower position to a higher position while receiving heat. Compared with other passive cooling devices such as loop heat pipes which have wick structures for the fluid suction, it is not necessary to use the wick structure for the heat driven pumps. The ideal working principle is shown in Figure 11, in which the inlet beaker has lower position while the outlet beaker has higher position. The horizontal branch is the heat receiving component while the other vertical branches are exposed in the air environment directly. Our previous paper (Xu and Shi, 2005; [7]) gives two criteria which govern the fluid discharge and liquid suction. Such criteria are summarized here to identify the working principle of the heat driven pumps. Considering the heat driven pump as an isolated system with both of the two check valves closed. Outside of the two beakers have the environment pressure p_{air}. Boiling in the horizontal section yields a positive pressure change rate while the condensation heat transfer in the vertical discharge branch yields the negative pressure change rate. The simple theoretical analysis shows that the initial bubble nucleation in the horizontal branch with full of liquid yields the higher positive pressure change rate. The other extremity is the smaller positive pressure change rate when the horizontal branch is full of vapor. When the above two pressure change rates are coupled with the negative pressure change rate taking place inside the vertical discharge branch, gives the fluid discharge criterion and the liquid suction criterion, respectively. The final fluid discharge and suction criteria can be expressed in the following form:

$$Q_{boil} > Q_{con} > C_1 C_2 Q_v \quad (2)$$

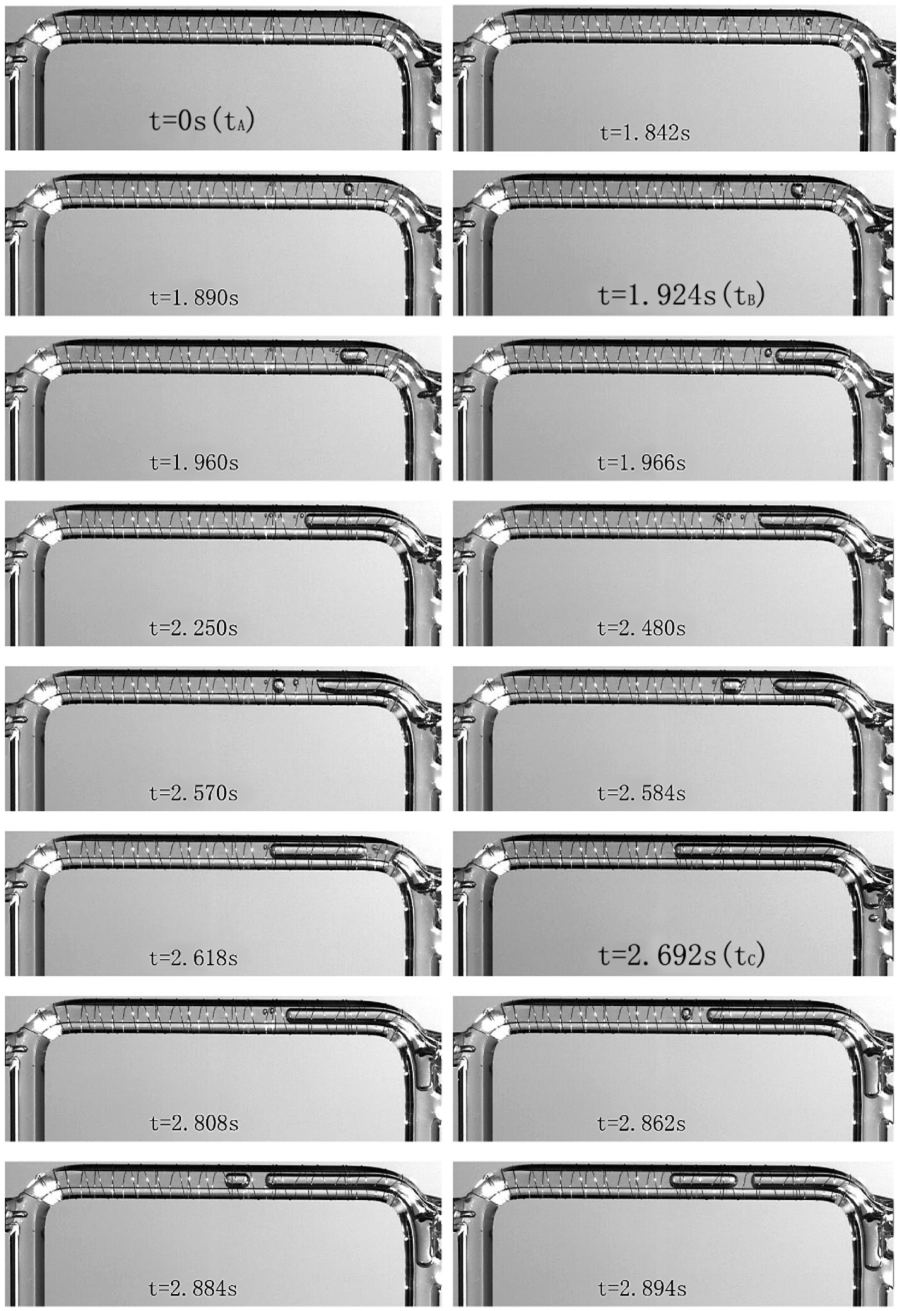

Figure 9. High-speed flow visualization of the inverted U-shaped heat driven pump at the heating power of 20 W (*continues*).

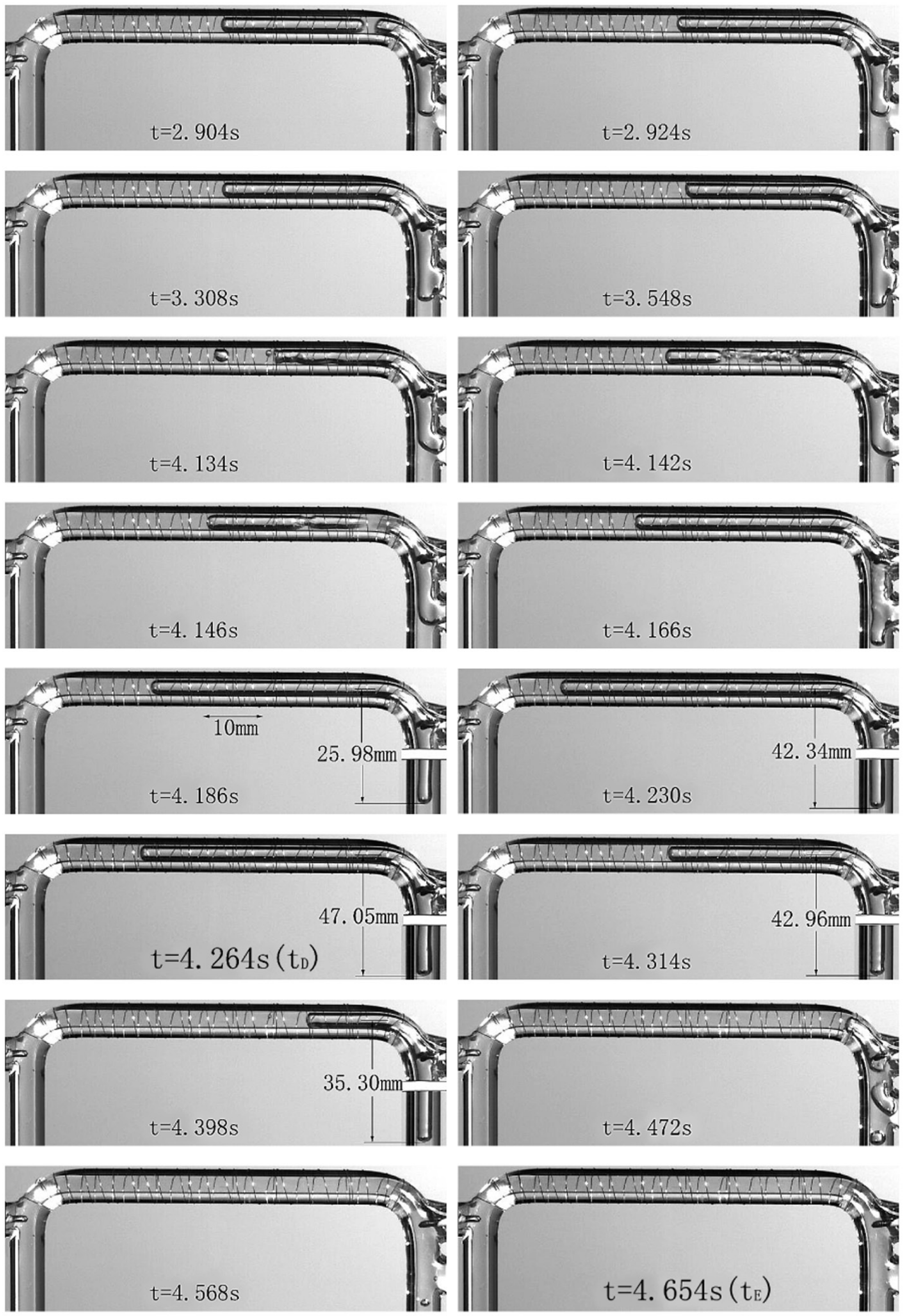

Figure 9. (*Continued*)..

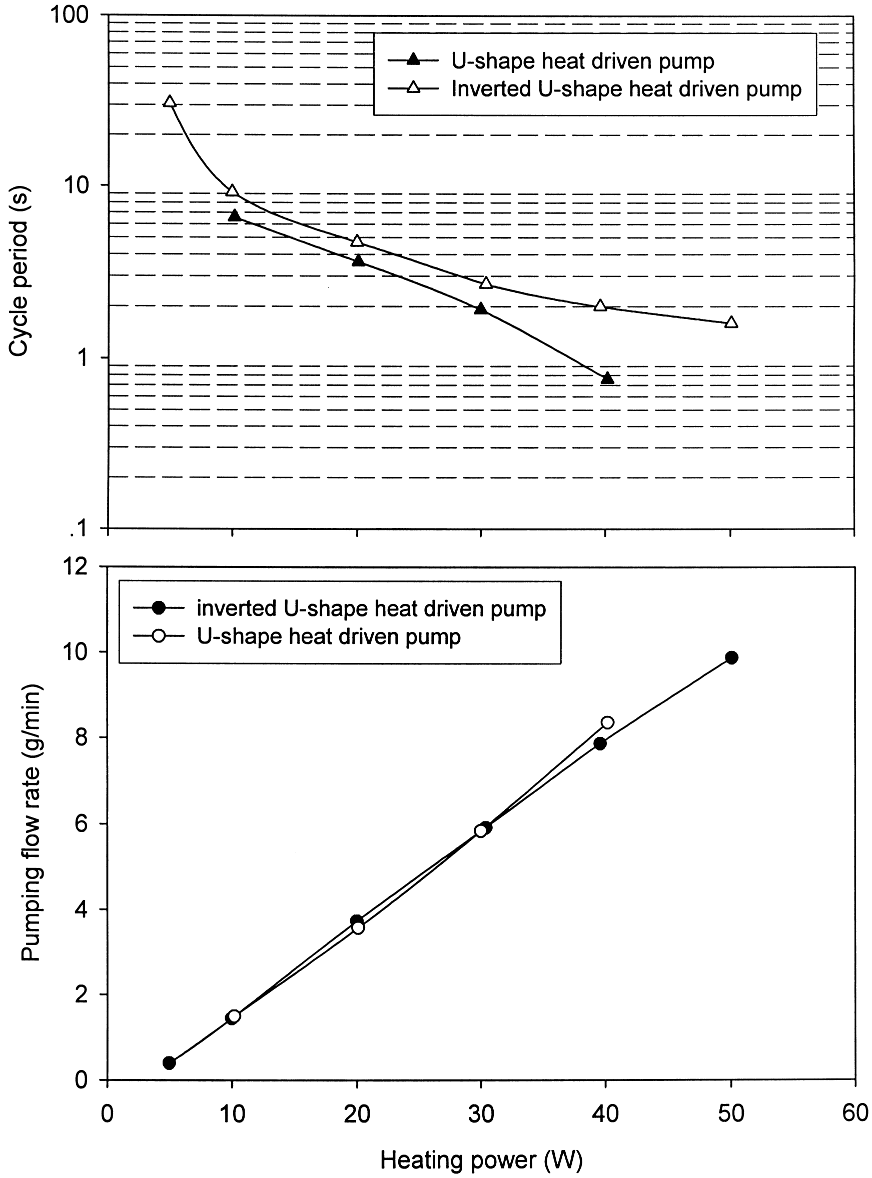

Figure 10. Cycle periods and pumping flow rates for both heat driven pumps.

where $C_1 = rR/a_v^2 C_{p,v}$, representing the physical properties of the working fluid, r, R, a_v, and $C_{p,v}$ are the latent heat of evaporation, gas constant, sound speed of the vapor, and specific heat of vapor, respectively. $C_2 = (V_{boil} + V_{con})/V_{boil}$, indicating the geometry configuration effect. V_{boil} and V_{con} are the inside volumes of the horizontal branch and the vertical discharge branch, respectively. Q_{boil}, Q_{con}, and Q_v are the boiling heat transfer rate in the horizontal branch, condensation heat transfer rate in the vertical discharge branch, and the single phase vapor heat transfer rate in the horizontal branch,

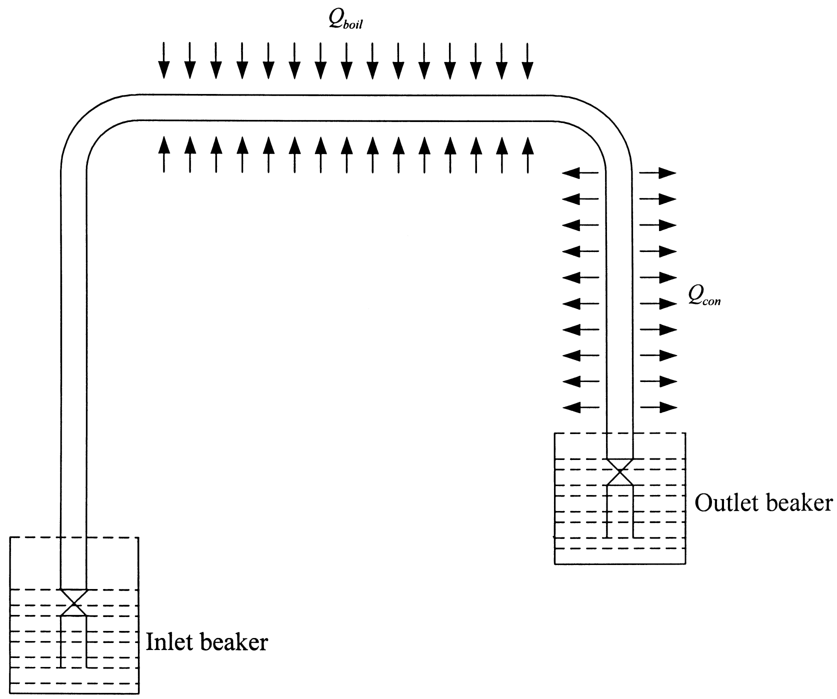

Figure 11. Ideal heat driven pumps demonstrating the working principles.

respectively. The combined criterion given in Eq. (2) indicates that the boiling heat transfer rate should be larger than the condensation heat transfer rate, thus the positive pressure can be accumulated inside the heat driven pump to initiate the open of the discharge check valve. On the other hand, the single phase vapor heat transfer rate should be smaller than the condensation heat transfer rate by $1/C_1C_2$ times thus negative pressure can be accumulated inside the heat driven pumps to initiate the fluid suction. Eq. (2) is the scaling law governing the working principle of the heat driven pumps. The present design satisfies the criteria given in Eq. (2) thus it can function as the heat driven pumps.

5. CONCLUSIONS

High speed flow visualization and dynamic measurements of heat driven pumps using both U-shaped and inverted U-shaped capillary tubes were performed. The following conclusions can be drawn:

1. The heat driven pumps using U-shaped capillary tube display the periodic working process. At the high heating powers, it behaves a successive of tiny bubble nucleation, growth, and coalescence process. Once the spherical bubble with the diameter reaching the inside diameter of the capillary tube, it expands quickly and the bubble slug forms, leading to a sharp positive pressure pulse. When the advancing vapor/liquid interface of the bubble slug reaches the highest position

in the vertical discharge branch, the condensation heat transfer between the saturated vapor and the subcooled liquid shrinks the bubble slug. Thus a negative pressure pulse is followed by the positive pressure pulse, causing the fresh liquid sucked into the system.

2. Heat driven pumps using the U-shaped capillary tube at the low heating powers display the similar process. However, in each full cycle, a set of positive pressure pulses are identified, corresponding to the new bubble nucleation, growth, and coalescence process in each substage. The newly formed bubble slug will chase the "old" one and the two bubble slugs are merging together. Only at the last substage, a negative pressure pulse is followed by the positive pressure pulse.
3. During the above bubble slug coalescence process, the liquid bridge between the two bubble slugs is deformed. The gravity force of the liquid bridge pulls the liquid down on the bottom of the horizontal capillary tube. When the two bubble slugs are thoroughly merging, a wave vapor/liquid interface is formed.
4. Heat driven pumps using the inverted U-shaped capillary tube demonstrate less number of substages in a full cycle. Besides, the wave vapor/liquid interface along the bottom of the horizontal capillary tube is never observed.
5. The cycle periods are decreased with increasing the heating powers, while the pumping flow rates are increased with increasing the heating powers linearly. The pumping performance of the two test sections show little differences, indicating that the gravity force has no apparent effect on the pumping performance. The gravity force only affects the vapor/liquid structure inside the pumping loop.

ACKNOWLEDGMENTS

This work is supported by the National Natural Science Foundation of China (50476088), Natural Science Foundation of Guangdong Province (32700), and the Science and Technology Development Foundation of Guangdong Province (33103).

REFERENCES

1. T. Yamamoto, Y. Takamura, and M. Katsuta, Study of Heat Driven Pump, *J. Fuel Soc. Jpn.*, vol. 59, no. 644, pp. 1016–1024, 1980.
2. T. Yamamoto, Y. Takamura, and M. Katsuta, Study of Heat Driven Pump, *J. Fuel Soc. Jpn.*, vol. 12, no. 1, pp. 19–24, 1982.
3. Y. Takamura, T. Yamamoto, and M. Katsuta, Proposal Heat Driven Pump for Heat Device, *Proceedings of the International Conference on Energy and Environment*, p. 538, May 1995.
4. Y. Takamura, T. Yamamoto, S. Matsumoto, and M. Katsuta, Development of Downward Heat Pipe Using Principle of Heat Driven Pump, in K. Chen, G. Sarlos, and T. W. Tong (eds.), *Proceedings of the International Conference on Energy and Environment*, Shanghai, China, May 1998.
5. J. L. Xu, X. Y. Huang, and T. N. Wong, Study on Heat Driven Pump, Part 1—Experimental Measurements, *International Journal of Heat and Mass Transfer*, vol. 46, pp. 3329–3335, 2003.
6. J. L. Xu, T. N. Wong, and X. Y. Huang, Study on Heat Driven Pump, Part 2—Mathematical Modeling, *International Journal of Heat and Mass Transfer*, vol. 46, pp. 3336–3347, 2003.
7. J. L. Xu and X. Shi, Pumping Criterion and Dynamic Measurements of an Inverted U-Shape Heat Driven Pumps Using Microchannels and Miniature Check Valves, *Experimental Thermal and Fluid Science*, vol. 29, pp. 579–590, 2005.